# Radio-frequency response of semiconducting CdF2:In crystals with Schottky barriers

**A. S. Shcheulin, A. K. Kupchikov, A. E. Angervaks, D. E. Onopko, A. I. Ryskin, A. I. Ritus, Artem V. Pronin, A. A. Volkov, Peter Lunkenheimer, Alois Loidl**

**Angaben zur Veröffentlichung / Publication details:**

Shcheulin, A. S., A. K. Kupchikov, A. E. Angervaks, D. E. Onopko, A. I. Ryskin, A. I. Ritus, Artem V. Pronin, A. A. Volkov, Peter Lunkenheimer, and Alois Loidl. 2001. "Radio-frequency response of semiconducting CdF2:In crystals with Schottky barriers." *Physical Review B* 63 (20): 205207. https://doi.org/10.1103/PhysRevB.63.205207.



# Radio-frequency response of semiconducting $CdF_2$:In crystals with Schottky barriers

A. S. Shcheulin, A. K. Kupchikov, A. E. Angervaks, D. E. Onopko, and A. I. Ryskin
*S.I. Vavilov State Optical Institute, 12 Birzhevaya Line, 199034 St. Petersburg, Russia*

A. I. Ritus, A. V. Pronin, and A. A. Volkov
*Institute of General Physics, Russian Academy of Sciences, 38 Vavilov Street, 117942 Moscow, Russia*

P. Lunkenheimer and A. Loidl
*Experimentalphysik V, Institut für Physik, Universität Augsburg, D-86135 Augsburg, Germany*
(Received 20 November 2000; published 2 May 2001)

The dielectric response of semiconducting $CdF_2$ crystals with bistable In centers in the range of $10^1 - 10^6$ Hz reveals a quasi-Debye relaxation due to Schottky barriers at the Au/Ag contacts. These spectra can be modeled with a two- or tri-layer capacitor, the characteristics of which are determined by the conductivity and capacity of the crystal volume and the depletion layers at the contacts (the Maxwell-Wagner capacitance). Analyses of the temperature dependence of these parameters show that the volume conductivity is due to free-electron motion, whereas the depletion-layer conductivity probably is caused by electron jumps over the deep In centers. Illumination of the crystals in the photoionization absorption band of the deep centers has the same effect upon the dielectric response as an increase of the temperature since both factors increase the free-electron concentration.

DOI: 10.1103/PhysRevB.63.205207 PACS number(s): 72.80.Jc, 77.22.Ch, 77.22.Gm

## I. INTRODUCTION

Semiconducting $CdF_2$:Ga and $CdF_2$:In crystals have gained growing interest as holographic media providing a new mechanism for photosensitivity caused by a change in the bistable center state.[1–5] These centers are identical to the DX-centers in conventional III–V and II–VI semiconductors.[6–10] They have two states: a shallow donor state and a two-electron deep state. The latter is characterized by a large lattice relaxation, in other words, by a large shift in the configuration coordinate, due to which a barrier arises between this and the shallow donor state. This barrier determines the metastable nature of the shallow state. For In, this barrier is very low ($<0.1$ eV), whereas for Ga it is record high for this class of crystals (around 1 eV).[5,6,10] The microscopic nature of the large lattice relaxation in $CdF_2$:Ga and $CdF_2$:In has been determined in Ref. 11. It consists predominantly in the displacement of the impurity ion along the forth-order axis into the nearest interstice. Such structure of the deep center was supported by recent positron annihilation studies[12] showing an open-volume defect, i.e., essentially, the presence of the cation vacancy in the structure of the center.

The giant band gap of the highly ionic cadmium fluoride crystal of $\sim$7.8 eV, together with relatively large binding energies of both states of the bistable center, make $CdF_2$:Ga and $CdF_2$:In an ideal model system for studying the DX centers and their interaction with electromagnetic radiation. In the present paper we describe the dielectric response of $CdF_2$:In in the frequency range of $10^1 - 10^6$ Hz. It is shown that this response can be described with simple models, which provide significant information on the DX centers in this material (see also Ref. 13).

## II. SAMPLES AND EXPERIMENTAL TECHNIQUE

$CdF_2$:In crystals were grown from the melt with the modified Stokbarger-Bridgmen technique. In dopant was introduced in the raw material for the growth in form of $InF_3$. Compensation of the surplus dopant charges (+1) was realized by interstitial $F^-$ ions. To convert the crystals into the semiconductor state, as-grown crystals were annealed in (Cd+K) vapors (an additive coloration of the crystals). Annealing results in the flow of fluorine ions from the bulk of the crystal to its surface, the charge compensation being provided by electrons coming from the surface and supplied by a reduction agent (Cd). Unlike the alkali-earth fluorides with fluorite structure and doped with column-III elements, M, in $CdF_2$:M the additional electrons, if they are not excited into the conduction band, are localized at the hydrogenic orbital, forming a neutral donor center ($M^{3+} + e_{hydr}$), rather than at atomiclike orbitals of the impurity yielding a different valence state ($M^{3+} \rightarrow M^{2+}$). However, for bistable Ga and In dopants, in addition to the two possible states of the impurity, namely the optically and electrically ''silent'' ionized state ($M^{3+}$) and the shallow donor state, the two-electron deep state ($M^{1+}$) is also possible.

The studies of the microwave and far-infrared absorption of semiconducting $CdF_2$:M crystals testifies to the presence of the interstitial $F^-$ ions, which cannot be fully removed from the crystal during coloration.[14] Probably, this is due to the occurrence of impurity-fluorine clusters together with statistically distributed M ions. Such clusters, perfectly embedded within the crystal matrix, are typical for the alkali-halide fluorides with fluorite structure and doped with M impurities.[15,16] These clusters are responsible for the giant solubility of many M dopants in fluorite-type crystals (for instance, $In_2F_3$ solubility in $CdF_2$ reaches $\sim$15 mole %.[17])

 

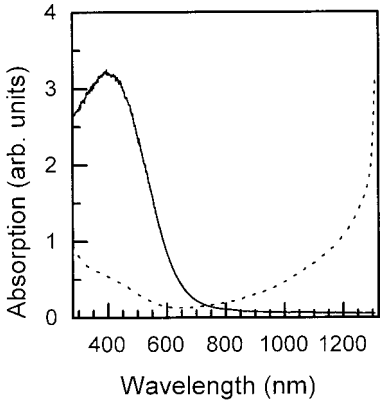


FIG. 1. Absorption spectra of $CdF_2$:In cooled in the dark (solid line) and illuminated in the UV-visible band (dotted line). Only the short-wavelength tail of the IR band with $\lambda_{max}=7\,\mu$m is shown.

Starting from a finite concentration of the M impurity of ~0.1 mole %, the further increase of M dopants predominantly results in the formation of clusters. Decay and formation of the clusters during annealing of the crystal at its concomitant coloration is a source of $F^-$ ions, which provides their presence in the colored crystal (as well as the corresponding quantity of $M^{3+}$ ions). The above considerations show that $F^-$ ions in the ionic semiconductor $CdF_2$ act in a similar way as acceptors in conventional semiconductors: they partly compensate the donor impurities. The total concentration of statistically distributed donor impurities, $N_M$, is larger than the concentration of the electrons introduced in the crystal during the coloration procedure, $n^*$, by the concentration of $F^-$ ions, $N_F$:

$$N_M = n^* + N_F. \tag{1}$$

To estimate $n^*$, the colored crystals were cooled to liquid helium temperature, at which all electrons introduced *via* coloration are bound at the deep centers, and illuminated with a ultraviolet-visible (UV-VIS) light, that corresponds to the photoionization absorption band of these centers (Fig. 1). This procedure converts the deep In centers into shallow donor (hydrogenic) centers according to the reaction shown in Eq. 2, which proceeds with a quantum yield of 2:[6]

$$\mathrm{In}^{1+} + \mathrm{In}^{3+} + h\nu \rightarrow 2(\mathrm{In}^{3+} + e_{\mathrm{hydr}}). \tag{2}$$

Upon this procedure, the UV-VIS band disappears and an infrared (IR) band, which corresponds to the photoionization of the shallow centers, arises (Fig. 1). The counting of number of quanta necessary for the total deep-to-shallow center conversion allows to find the total number of deep centers in the sample and their concentration, $N_d^-$, which is equal under these conditions to $(1/2)n^*$ (here and below, the upper index in the In center concentration shows the center charge with respect to cation).

The bulk of the experiments has been performed using two crystals with $InF_3$ concentrations in the raw material of 0.02 and 0.5 mole %. Taking into account the distribution coefficient of In in $CdF_2$ is equal to 0.31 (Ref. 18) one can estimate the average In concentration in these crystals as $\sim 1.7\cdot 10^{18}\,\mathrm{cm}^{-3}$, and $4.2\cdot 10^{19}\,\mathrm{cm}^{-3}$, respectively [there are parts of the crystals with smaller (lower part) and larger (upper part) concentration compared with the average concentration]. For the former crystal (sample 1) the use of above technique gives $n^* = (3.5\pm 0.7)\cdot 10^{18}\,\mathrm{cm}^{-3}$ (the sample was cut out of the upper part of the crystal).

For the second crystal, using two different coloration regimes results in samples with $n^* = (2.0\pm 0.4)\cdot 10^{18}\,\mathrm{cm}^{-3}$ (''soft'' regime, sample 2a) and $n^* = (5.0\pm 1.0)\cdot 10^{18}\,\mathrm{cm}^{-3}$ (''hard'' regime, sample 2b). Further increase of coloration time, Cd pressure, or temperature did not give a noticeable increase of $n^*$ as compared to sample 2b. Consequently, the majority of In ions in this crystal are bound in clusters and only a small fraction is statistically distributed over the bulk of the crystal and only these ions can be reduced.

A total concentration of statistically distributed ions, $N_{\mathrm{In}} = n^* + N_F$ in the samples cannot be evaluated since the latter quantity, $N_F$, is unknown.

It was found that as-grown $CdF_2$:In crystals are weakly reduced already during the growth process[19] so, the dielectric response of the as-grown crystal 2 was also studied (sample 2c; in this case, $n^*$ was so small that a determination with the technique mentioned above was not possible). A pure $CdF_2$ sample was also studied as a reference system.

To study the radio-frequency response of the crystals, the samples have been prepared in the form of plane-parallel plates with area, $S = 20\,\mathrm{mm}^2$. The thickness of the plates was $d = 0.47$ mm for sample 1 and 1.3–1.5 mm for samples 2. The samples have been polished and treated after polishing with concentrated HCl to eliminate the surface layers. Gold or silver contacts of 5–10 $\mu$m thickness have been deposited on opposite sides of the plates by plasma sputtering.[20]

Along with the deposition of Au/Ag contacts directly on the crystal surface, mica linings with a thickness of 10–35$\mu$m were introduced between contacts and crystal. Teflon linings with a thickness of 55$\mu$m were also used; in this case, polished brass electrodes were used. Wires were glued to the Au/Ag or brass electrodes with conducting glue.

The samples were mounted on the cold finger of a He-flow cryostat with windows enabling their illumination. Wires from the samples were soldered to transition terminals of the cryostat. To measure the impedance $Z$ of the sample, these terminals were included in one of the shoulders of a bridge scheme of the analyzer, with which an equivalent capacity $C_p$ of the sample and equivalent conductivity $G_p (Z^{-1} = G_p + i\omega C_p)$ were measured in the temperature range of 77–315 K. The alternating voltage at the contacts was sufficiently small to neglect its influence on the balance conditions. The resulting data are presented as $C_p$ and loss tangent, $\mathrm{tg}\delta = G_p/(\omega\cdot C_p)$. In addition, the response of crystals illuminated either with a mercury high-pressure lamp through a combination of filters picking up the UV-VIS range or with an argon laser ($\lambda = 488$ nm) was studied.

## III. EXPERIMENTAL RESULTS AND DISCUSSION

### A. Dielectric response of the crystals

The frequency dependence of $C_p$ and tg $\delta$ for samples 1 and 2, utilizing gold electrodes, is presented in Figs. 2–5 for

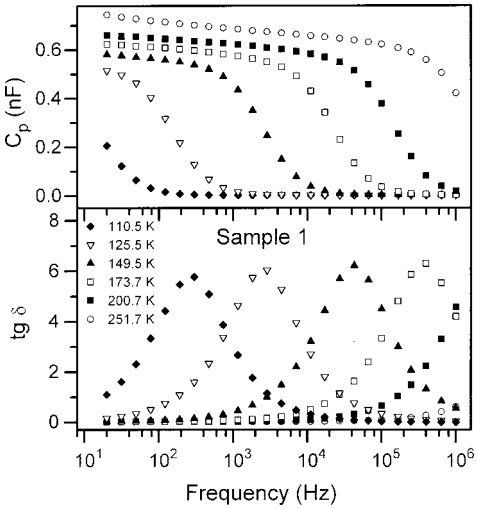


FIG. 2. Capacitance (upper frame) and loss tangent (lower frame) of $CdF_2$:In (sample 1 with Au contacts; $n^*=3.5\times10^{18}$ $cm^{-3}$) vs frequency for different temperatures.

a series of temperatures. Sample 1 reveals an almost ideal Debye-type of relaxation except for a slight increase of the dielectric constant towards low temperatures (Fig. 2). The low-temperature response ($T<200$ K) of samples 2a and 2b reveals a very similar characteristic. The loss angle of sample 2b strongly increases towards low frequencies. For temperatures $T>200$ K, indications of a second Debye relaxation show up in the spectra: a second low-frequency plateau and a second maximum in tg $\delta$. For sample 2b, the second maximum in the loss angle is masked by the aforementioned strong increase in tg $\delta$ towards low frequencies. Figure 6 shows the effect of illumination as observed in sample 2b at 90 K. Here the dielectric response as observed in the dark is compared to that as observed under UV-VIS illumination. At this point we can give a preliminary summary of the results: (i) With increasing $n^*$ the primary Debye relaxations are shifted to higher frequencies, yielding a shift of the loss maximum and a concomitant shift of the step in the capacitance to higher frequencies. (ii) Spectra of all samples with

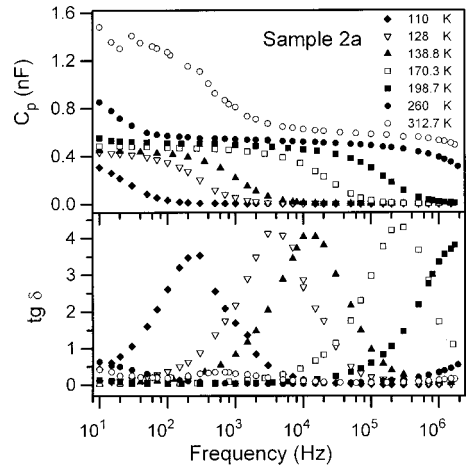


FIG. 3. Dielectric response of $CdF_2$:In (sample 2a with Au contacts, $n^*=2.0\times10^{18}$ $cm^{-3}$).

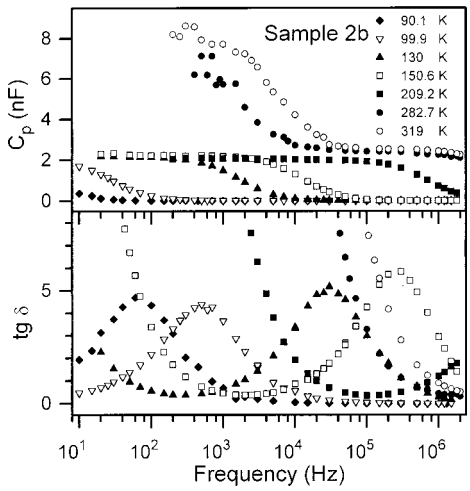


FIG. 4. Dielectric response of $CdF_2$:In (sample 2b with Au contacts, $n^*=5.0\times10^{18}$ $cm^{-3}$).

linings show one plateau in $C_p$ (the absolute value of which is smaller by two orders of magnitude) and one maximum in tg$\delta(\omega)$, shifted to higher frequencies as compared to the same sample without linings. This frequency shift reaches two orders of magnitude. (iii) The dielectric response of the undoped sample reveals a weak spectral dependence only. (iv) The illumination of samples 1 and 2 at low temperatures results in spectra similar to those observed at elevated temperatures: illumination has the same effect as thermal heating. The effect of illumination vanishes at elevated temperatures.

### B. Equivalent circuit analysis of the experimental results

The semiconducting sample with insulating linings may be considered as a two-layer Maxwell-Wagner capacitor, Fig. 7(a). Its response to an ac electric field is determined by an impedance

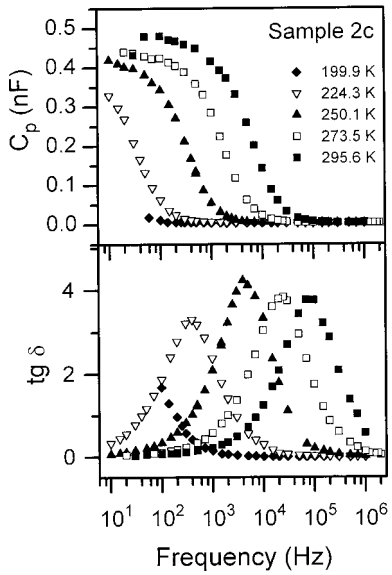


FIG. 5. Dielectric response of $CdF_2$:In (sample 2c with Au contacts).

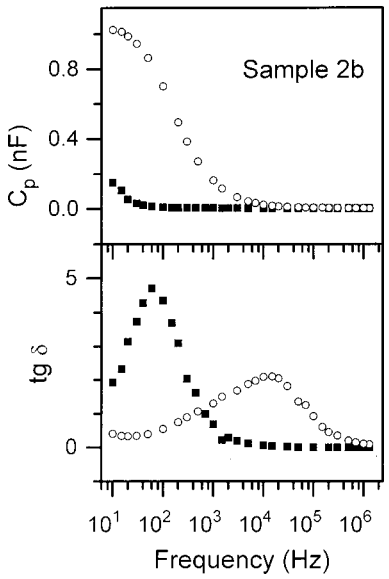


FIG. 6. Dielectric response of $CdF_2$:In (sample 2b with Au contacts, $T=90.1$ K) in the darkness (full squares) and under UV-VIS illumination (open circles).

$$Z(\omega)=Z_1(\omega)+Z_2(\omega), \tag{3}$$

where

$$\frac{1}{Z_1}=\frac{1}{R_1}+i\omega C_1,$$

$$\frac{1}{Z_2}=\frac{1}{R_2}+i\omega C_2. \tag{4}$$

Index ''1'' refers to the crystal and index ''2'' refers to the linings ($C_2$ equals 1/2 of the capacity of each lining). It is shown in Ref. 21 that such a two-layer capacitor can be considered as a homogeneous sample with an effective dielectric permittivity $\varepsilon=\varepsilon'+i\varepsilon''$, where

$$\varepsilon'=\varepsilon_\infty\left(1+\frac{\chi}{1+\omega^2\tau^2}\right), \tag{5}$$

$$\varepsilon''=\varepsilon_\infty\left(\frac{\tau}{\omega\tau_1\tau_2}+\frac{\chi\omega\tau}{1+\omega^2\tau^2}\right). \tag{6}$$

Here,

$$\chi=\frac{\varepsilon_s-\varepsilon_\infty}{\varepsilon_\infty},\quad \tau_1=R_1C_1,\quad \tau_2=R_2C_2,$$

and

$$\tau=\frac{R_1\tau_2+R_2\tau_1}{R_1+R_2}.$$

Indexes ''$s$'' and ''$\infty$'' refer to zero and infinitely high frequencies, respectively, i.e., to the static and the optical permittivity. Those are connected to the parameters of the two-layer capacitor by

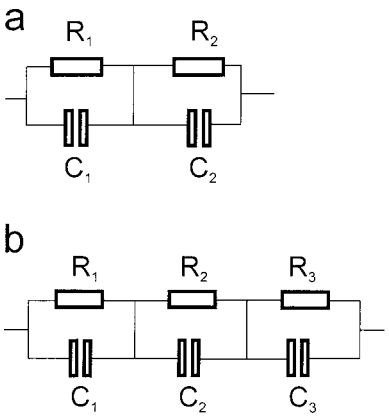


FIG. 7. Equivalent circuits of the two-layer (a) and the trilayer (b) dielectric cells, which model the dielectric response of $CdF_2$:In crystals.

$$\varepsilon_s=\frac{1}{C_0}\frac{R_1\tau_1+R_2\tau_2}{(R_1+R_2)^2}\quad\text{and}\quad \varepsilon_\infty=\frac{1}{C_0}\frac{\tau_1\tau_2}{R_1\tau_2+R_2\tau_1},$$

with $C_0$ the geometrical capacitance of the sample. It is seen from Eqs. (5) and (6) that the relaxation spectrum of a two-layer capacitor coincides with the spectrum of a Debye relaxator including an additional term due to the ohmic conductivity [the first term in Eqn. (6)].[21] This similarity should be, however, considered as a formal one since the Maxwell-Wagner spectra describe the purely macroscopic effect of interlayer polarization, whereas the Debye spectra result from relaxations of microscopic dipoles.

The similarity of the relaxation spectra of samples with and without linings indicates the existence of depletion layers near the Au/Ag electrodes. They arise from the difference of the Fermi levels in the crystal and in the metal leading to the formation of Schottky barriers. The depletion layers are responsible for the relatively large low-frequency capacitance of the object under investigation—the sample plus two electrodes. Hence, one may use the equivalent circuit shown in Fig. 7(a) as a model system to describe crystals with depletion layers.

Using $G_i=1/R_i$ and $C_i$ ($i=1$, 2 refer to the sample and to the depletion layer, respectively) as fit parameters, Eqs. (5) and (6) allow to calculate the frequency dependence of the complex capacitance of the cell and to compare it to the experimentally observed $C_p(\omega)$ and $G_p(\omega)/\omega=\mathrm{tg}\,\delta\cdot C_p(\omega)$. Figure 8 demonstrates the good quality of such a fit for sample 2a except for the small increase towards low frequencies of $C_p(\omega)$ and the too shallow increase of $G_p(\omega)/\omega$ at low frequencies, which both cannot be described by the fit. $C_2$ was found to be approximately two orders of magnitude higher as compared to $C_1$; their ratio characterizes a relative thickness of the depletion layer that occurs to be less than 1.0% of the crystal thickness and is essentially thinner than the linings used. Both $C_1$ and $C_2$ weakly depend on $T$, unlike $R_1$ and $R_2$, $R_2$ exceeding $R_1$ by several orders of magnitude.

Figure 9 shows an Arrhenius plot for $G_1(T)$ of sample 1, deduced from the fits with $R_2=\infty$. The plot $\lg G_1$ vs $1/T$ shows a significant linear dependence for temperatures

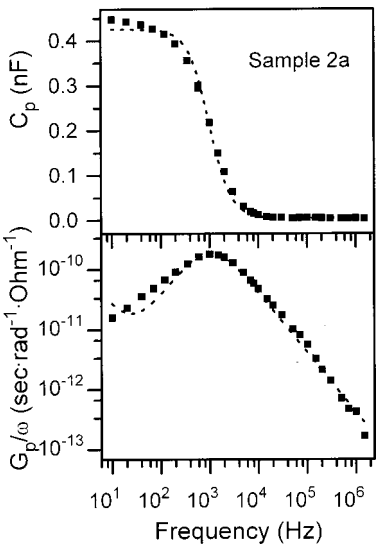


FIG. 8. Fitting of the dielectric response of sample 2a at 138.8 K with a two-layer model (dotted line).

$130\,\mathrm{K} \leqslant T \leqslant 230\,\mathrm{K}$, with an activation energy, $E_{ac}$ of $(0.197 \pm 0.008)$ eV. It should be stressed that $G_1$ has the same values for this sample with and without linings, which proves the high reliability of the model used.

Samples 2a and 2b can be described by a two-layer model for low temperatures only. At higher $T$, an additional low-frequency step in $C_p(\omega)$ and an additional low-frequency maximum in $\mathrm{tg}\,\delta(\omega)$ appear. One may suppose to describe these additional features *via* an additional ''even more depleted'' layer (Fig. 7b, $R_3 > R_2 > R_1$). Thus, two new fit parameters, $R_3$ and $C_3$ should be introduced. The trilayer model describes all the spectral features of the samples 2a and 2b though some quantitative discrepancies remain (Fig. 10). Arrhenius plots of $G_1(T)$ for these samples show a linear dependence in the same temperature range as for sample 1. The activation energy is $(0.20 \pm 0.01)$ eV for sample 2a and $(0.19 \pm 0.01)$ eV for sample 2b. In the temperature range $T > 200\,\mathrm{K}$, where the second step in $C_p(\omega)$ and the second maximum in $\mathrm{tg}\,\delta(\omega)$ arise, reliable values of the parameter $R_2$ can be found. Arrhenius plots of $G_2(T)$ for samples 2a

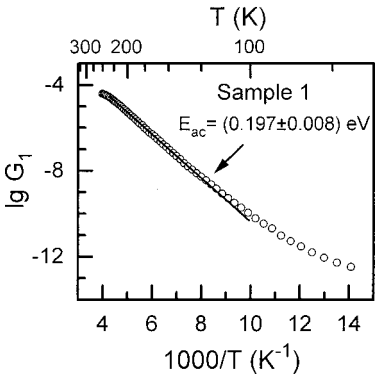


FIG. 9. Arrhenius plot of the volume conductivity $G_1$ of the sample 1 composed from many fits by the two-layer model.

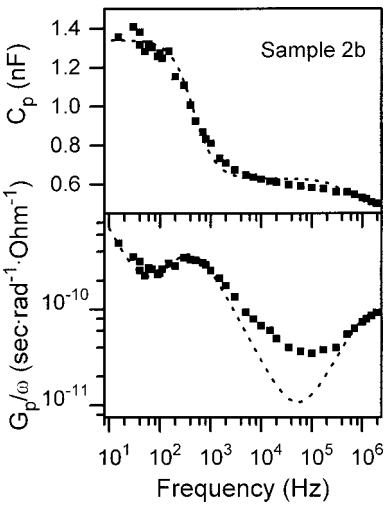


FIG. 10. Fitting of the dielectric response of the sample 2a at 312.7 K with the trilayer model (dotted line).

and 2b show in this range a linear dependence with equal activation energy of $(0.24 \pm 0.01)$ eV. The resistance $R_3$ is very high and no clear information on its temperature dependence could be obtained (as well as for $R_2$ in the two-layer model). The capacitances $C_2$ and $C_3$ occur to be of the same order of magnitude.

The strong increase in $\mathrm{tg}\,\delta(\omega)$ with a decrease of $\omega$ for sample 2b at $T > 150\,\mathrm{K}$ (Fig. 4) is due to the first term in Eq. 6 (the ohmic conductivity). This term is equal to $\omega^{-1}R_2^{-1}$ for $R_2 \gg R_1$, and therefore, Fig. 4 directly reveals a higher conductance of the depletion layer in sample 2b compared to sample 2a. The spectra of the noncolored sample 2c can be described with a two-layer model with relatively high-activation energy for $G_1(T)$ of $(0.42 \pm 0.01)$ eV.

Activation energies for all samples under investigation are summarized in Table 1.

### C. Distribution of electrons between In centers and conduction band

To confirm the proposal on the electronic nature of the response in $CdF_2$:In, we compare the temperature dependence of the conductivity, $G_1(T)$, to the calculated free-electron concentration, $n(T)$. In the following, $n(T)$ will be calculated in the framework of statistical considerations of the distribution of $n^*$ electrons, introduced in the crystal during coloration, between two levels of the bistable centers (or equivalently between two states, shallow and deep) and

TABLE I.

| Sample | $InF_3$ in raw material, mole % | $n^*$, $10^{18}\,\mathrm{cm}^{-3}$ | Volume $E_{ac}$, (eV) | Depletion layer $E_{ac}$, (eV) |
|---|---|---|---|---|
| 1 | 0.02 | $3.5 \pm 0.7$ | $0.197 \pm 0.008$ | |
| 2a | 0.5 | $2.0 \pm 0.4$ | $0.20 \pm 0.01$ | $0.24 \pm 0.01$ |
| 2b | 0.5 | $5.0 \pm 1.0$ | $0.19 \pm 0.01$ | $0.24 \pm 0.01$ |
| 2c | 0.5 | ~0.01 or less | $0.42 \pm 0.01$ | |

the conduction band. Similar considerations were made in Refs. 22, 23. However, there the incorrect assumption was made that, unlike DX centers in conventional semiconductors, the deep state of In is a single-electron state, i.e., an $In^{2+}$ state.[24] The problem can be solved in a manner similar to that for a double-charged donor,[25] but with an essential difference: whereas at 0 K each double-donor ion has two electrons, for the case in consideration only $n^*/2$ In centers per $cm^3$ contain two electrons and $[(n^*/2)+N_F]$ centers are empty, i.e., they are ionized. The concentrations of the statistically distributed impurities and of the electrons, introduced into the crystal at its coloration, may be expressed via the concentration of the shallow donors ($N_{sh}^0$), the ionized ($N_{sh}^+$), and the deep ($N_d^-$) centers and free-electron concentration ($n$) with Eqs. 7 and 8, respectively:

$$N_{In}=N_{sh}^+ + N_d^- + N_{sh}^0 \tag{7}$$

$$n^*=2N_d^- + N_{sh}^0 + n. \tag{8}$$

The balance equation for free electrons is given by:

$$n=N_{sh}^+ - N_d^- - N_F. \tag{9}$$

The analysis of the statistics of the electron distribution over shallow and deep centers and the conduction band leads to the following equation:

$$x^3+x^2(2\beta+\gamma+1)+x(\alpha\beta+2\gamma\beta)+\alpha\beta(\gamma-1)=0. \tag{10}$$

Here,

$$x=n/N_{In}=(n/N_0)\exp[-(E_0-E_F)/kT], \tag{11}$$

$$\gamma=N_F/N_{In}. \tag{12}$$

$$\alpha=(N_0/N_{In})\exp[(E'_{sh}-E_0)/kT], \tag{13}$$

$$\beta=(N_0/N_{In})\exp[(E'_d-E_0)/kT]. \tag{14}$$

In Eqs. (11), (13), and (14), the quantities $E_0$, $E'_{sh}$, $E'_d$, and $E_F$ denote the energies of the lower edge of the conduction band, the shallow level, the deep level, and the Fermi level, respectively. All those values are measured from an arbitrary zero level. $N_0$ is a density of states in the conduction band, given by:

$$N_0=2(2\pi m^* kT/h^2)^{3/2}. \tag{15}$$

The effective mass $m^*$ of electrons in $CdF_2$ is 0.45 of the free-electron mass[26] and the binding energies of the centers are: $E_{sh}=E_0-E'_{sh}$, $E_d=E_0-E'_d$. We note that the equations for $x$, $\alpha$, and $\beta$ [Eqs. (11), (13), (14)] differ by a factor of 2 from those given in Ref. 25.

The solution of Eq. (10) has been executed numerically, the root $x_0$ satisfying the condition $0<x_0<1$. After solving Eq. (10), the concentration of the shallow, deep, and ionized centers can be determined from the following ratios:

$$N_{sh}^0=2N_{In}f_{sh}(1-f_d)/(1+f_{sh}-f_d); \tag{16}$$

$$N_d^-=N_{sh}^0 f_d/2(1-f_d); \tag{17}$$

$$N_{sh}^+=N_{sh}^0(1-f_{sh})/2f_{sh}. \tag{18}$$

Here, $f_i(i=\mathrm{sh},d)$ are the Fermi functions:

$$f_{sh}=[(\alpha/x)+1]^{-1}, \tag{19}$$

$$f_d=[(\beta/x)+1]^{-1}. \tag{20}$$

The knowledge of $N_{sh}^+$, $N_d^-$, and $N_F$ allows to find $n$ from Eq. (9).

Important parameters, which determine predominantly the character of the temperature dependence of the electron concentrations, are the binding energies of the shallow and the deep centers. The technique for finding $E_{sh}$ via comparison of the experimental shape of the IR band to one calculated using a hydrogenic model of the shallow center, gives values of $E_{sh}$ for various column-III dopants of 0.10–0.12 eV.[27] We used $E_{sh}$ equal to 0.10 eV found for $CdF_2$:In by the thermoelectric effects spectroscopy (TES) technique.[28] For the energy $E_d$ we took a value of 0.25 eV, which was found in a first-principles study of the bistable Ga and In centers in $CdF_2$;[11] the same value was found by the TES techniques.[28]

The calculated temperature dependencies of $N_d^-$, $N_{sh}^+$, $N_{sh}^0$, and $n$ for the $CdF_2$:In crystal with $N_{In}=2\times10^{18}\,cm^{-3}$, $N_F\cong0$ are shown in Fig. 11. In the temperature range $40\,K<T<140\,K$ almost all electrons are localized at the deep centers and $N_d^-\approx n^*/2$. Above $T\approx140\,K$ the deep centers vanish *via* thermal activation, accompanied by the formation of shallow centers and free electrons. Arrhenius plots for $N_{sh}^0$ and $n$ reveal $E_{ac}=0.074\,eV$ for the former quantity and two very similar activation energies for the latter quantity: 0.185 eV for the 40–200 K range and 0.204 eV for the 200–500 K range. In Fig. 11(d) an ''averaged'' value $E_{ac}$ of 0.195 eV is indicated. Interestingly, the above activation energies have nothing to do with any binding energy of the In center, which is typical for a center having several states (levels). A change in $N_{In}$, $N_F$ has a weak influence on $E_{ac}(N_{sh}^0)$, $E_{ac}(n)$. On the contrary, these activation energies are very sensitive to the values of the binding energy of both centers, as well as to the density of states in the conduction band.

### D. Discussion of experimental results

A reasonable coincidence of the experimental and calculated frequency dependence for $C_p(\omega)$ and $G_p(\omega)/\omega$ (Figs. 8, 10) shows that the simple equivalent circuits presented in Fig. 7 describe sufficiently well the ''$CdF_2$:In crystal+Au/Ag contacts'' samples. At the moment, we cannot propose a physical model for the element 3 in Fig. 7(b); its occurrence testifies to a more complex nature of the potential relief at the contact. It is not excluded that this layer is due to a deep surface state.

The similar values of the activation energies in the temperature range $130\,K<T<230\,K$ of 0.19–0.20 eV found from the Arrhenius plots for $G_1(T)$ (samples 1, 2a, and 2b) and for the calculated $n(T)$, confirm the proposed mechanism of formation of the dielectric response due to the depletion layers.[29] This proposal is also supported by the very

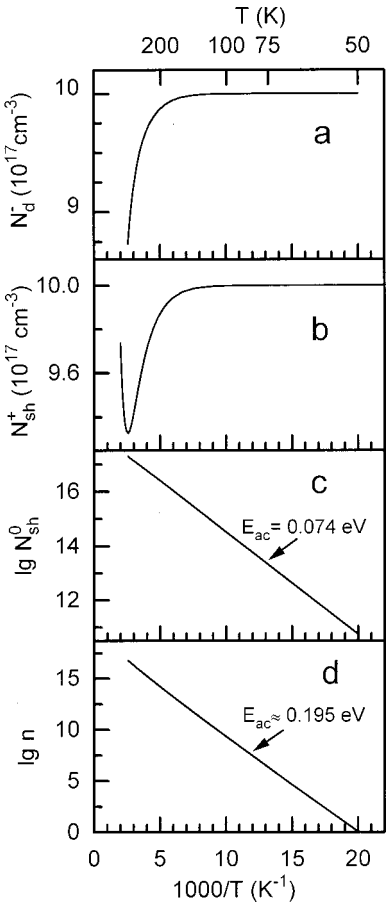


FIG. 11. Calculated concentrations of the deep (a), ionized (b), and shallow donor centers (c) and of the free-electron concentration (d) for the $CdF_2$:In crystal with $N_{In}=n^*=2\cdot10^{18}\,cm^{-3}$.

weak dependence of $E_{ac}$ on $n^*$, which is found in both the experimental studies and the statistical consideration [$n^*$ varies in our samples in the range of $(2.0–5.0)\cdot10^{18}\,cm^{-3}$].

It becomes clear from the above considerations that the quantity $G_1(T)$ reflects the free-electron conductivity of $CdF_2$:In. The question arises on the nature of $G_2$ and $G_3$, which are tied to the depletion layers (samples 2a and 2b). Attention should be paid to the closeness of the activation energy for $G_2$ found with the trilayer model (0.24 eV) and the binding energy of the deep In centers (0.25 eV).[11,28] One may suppose that the charge transport in the depletion layers is due to jump conductivity over the deep centers. In fact, at higher temperatures and for a sufficiently large difference in Fermi levels of the crystal and the contact, not only the conduction band will be depleted with the carriers, but also the shallow donor levels. In this case, only thermally induced jumps of electrons over deep centers in the depletion layer can contribute to the dielectric response of the crystal. Linearity of the Arrhenius plot for $G_2(T)$ at temperatures, at which deviations from linearity are clearly observed for $G_1(T)$, demonstrates that these jumps do not involve extended movement of the carriers; once escaped, electrons are captured immediately by one of the nearest ionized centers under the formation of a deep center. The electric field in the depletion layer is much smaller as compared to intra-atomic fields. Therefore, its presence cannot essentially disturb the binding energy of the deep center. Thus, an activation energy of 0.24 eV gives a reliable value of the binding energy of the deep center.

As mentioned above, for sample 1, $G_2(T)$ is too small to be detectable and reasonable fits of the frequency-dependent response can be obtained assuming $G_2=0$. Obviously, the conductivity of the depletion layer is much smaller in this sample than in samples 2a and 2b. One may suppose that this finding is predominantly due to the smaller jump mobility of electrons in the depletion layer, which decreases $G_2$ in this sample below the limit of detection. This mobility is determined by the concentration $N_{In}$, which should be essentially smaller in sample 1 as compared to sample 2. In addition, it was noted above that $G_2$ in sample 2b is considerably higher than in sample 2a. This may be attributed to the higher electron concentration $n^*$ introduced during coloration in sample 2b.

The similarity of the effect of illumination in the UV-VIS band and the temperature increase on the dielectric response confirms its electronic nature: both factors increase the concentration of free electrons, which leads to an increase of the volume conductance $G_1$. For the reasonable case of $R_2 \gg R_1$ and $C_2 \gg C_1$, the characteristic frequency $\omega=1/\tau$ of the relaxation features, observed in $C_p(T)$ and tg $\delta(\omega)$ [see Eq. (6)], can be approximated by $1/\tau \approx G_1/C_2$. Therefore, both an increase of temperature and an illumination of the sample will lead to a shift of the relaxation features to higher frequencies, in good agreement with the experimental observations.

The failure to observe the thermally stimulated depolarization phenomenon in the $Cd_{1-x}M_xF_{2+x}$ solid solution testifies clearly to a nonlocal mechanism of charge compensation in $CdF_2$.[30] Thus, the signal, induced in the as-grown $CdF_2$:In crystal (sample 2c) also is electronic, rather than ionic in nature. It is incomprehensible that the activation energy of the $G_1$ parameter in this sample is well above any characteristic energy of In centers in $CdF_2$. To explain this value, we suppose a small contamination of Ga (the same setup was used for a long time for growth of $CdF_2$Ga: crystals). To support this proposal, statistical considerations similar to those described above were made for this crystal with the following parameters: $N_{In}=1\times10^{19}\,cm^{-3}$, $N_{Ga}=1\times10^{16}\,cm^{-3}$, $n^*=1\times10^{16}\,cm^{-3}$, $E_d$ for Ga being 0.7 eV (Ref. 11) (see also Ref. 5). This calculation gives an almost linear dependence of $\lg n$ vs $1/T$, with an activation energy of ~0.4 eV. Thus, if the concentration of electrons introduced in the $CdF_2$:In crystals is comparable to the Ga trace concentration, the Ga deep centers with large binding energy can essentially lead to an increase of the effective activation energy of free electrons in this crystal. With the increase of $n^*$ all deep Ga levels are filled with electrons and cease to influence the statistics of the electron distribution.

## IV. CONCLUSION

The dielectric response of the ionic semiconductor $CdF_2$ with bistable In centers has been investigated in the frequency range $10^1–10^6$ Hz at temperatures 20–315 K. Silver

or gold electrodes form depletion layers near the surfaces of the samples (Schottky barriers), which leads to a Debye-like relaxation behavior. An analysis of this response can be performed in the framework of very simple models using equivalent circuits. This analysis allows us to determine the temperature dependence of the conductivity due to free carriers in the conduction band (volume conductivity) and of the jump conductivity over the deep In centers (conductivity in the depletion layers). The binding energy of the deep In centers derived from $T$ dependence of the depletion layer conductivity is close to this energy found in the first-principal calculation[11] and also in TES experiments.[28] This energy used as a parameter in statistical consideration of the distribution of electrons between the center levels and the conduction band gives a true $T$ dependence of the volume conductivity. Thus, the equivalent circuit analysis of the dielectric response of $CdF_2$:In gives self-consistent results. This analysis clearly indicates the presence of traces of Ga contamination in the investigated $CdF_2$In crystals.

Illumination of the crystals in the UV-VIS absorption band influences the dielectric response in the same manner as a temperature increase. The dynamic nature of the photoinduced metastable state in $CdF_2$:In at $T>40$ K does not allow, however, for a detailed investigation of the temperature dependence of the photoinduced response, since it is impossible to separate the temperature and the illumination effects. Such a study can be performed for Ga impurities due to a much higher barrier separating the metastable and the ground state ($\sim$1 eV) and the essentially higher temperature, at which the photoinduced shallow state is stable ($\sim$200 K).

This study shows that dielectric spectroscopy in the audio- and radio-frequency range is an effective tool for studies of deep centers in semiconductors.

## ACKNOWLEDGMENTS

We are indebted to I. I. Buchinskaya, P. P. Fedorov, and B. P. Sobolev for the crystal growth. The research was partly supported by the CRDF under the Grant No RP1-2096 and by the German BMBF under the Grant No. EKM 13N6917.

[1] A. I. Ryskin, A. S. Shcheulin, B. Koziarska, J. M. Langer, A. Suchocki, I. I. Buchinskaya, P. P. Fedorov, and B. P. Sobolev, Appl. Phys. Lett. **67**, 31 (1995).

[2] B. Koziarska, J. M. Langer, A. I. Ryskin, A. S. Shcheulin, and A. Suchocki, Acta Phys. Pol. A **88**, 1010 (1995); Mater. Sci. Forum **196–201**, 1103 (1995); A. Suchocki, B. Koziarska, T. Langer, and J. M. Langer, Appl. Phys. Lett. **70**, 22 (1997).

[3] A. I. Ryskin, A. S. Shcheulin, E. V. Miloglyadov, R. A. Linke, I. Redmond, I. I. Buchinskaya, P. P. Fedorov, and B. P. Sobolev, J. Appl. Phys. **83**, 2215 (1998).

[4] A. Nahata, C. J. DiCaprio, H. Yamada, A. I. Ryskin, A. S. Shcheulin, and R. A. Linke, IEEE Photonics Technol. Lett. **12**, 1525 (2000).

[5] R. A. Linke, A. S. Shcheulin, A. I. Ryskin, I. I. Buchinskaya, P. P. Fedorov, and B. P. Sobolev, Appl. Phys. B: Lasers Opt. (to be published).

[6] A. S. Shcheulin, A. I. Ryskin, K. Swiatek, and J. M. Langer, Phys. Lett. A **222**, 107 (1996).

[7] S. A. Kazanskii, A. I. Ryskin, and V. V. Romanov, Appl. Phys. Lett. **70**, 1272 (1997); Phys. Solid State **39**, 1067 (1997).

[8] A. I. Ryskin and P. P. Fedorov, Phys. Solid State **39**, 943 (1997).

[9] A. I. Ryskin, A. S. Shcheulin, and D. E. Onopko, Phys. Rev. Lett. **80**, 2949 (1998); A. S. Shcheulin, A. I. Ryskin, and D. E. Onopko, Phys. Solid State **39**, 1906 (1997).

[10] A. I. Ryskin and D. E. Onopko, Phys. Rev. B **61**, 12 952 (2000).

[11] C. H. Park and D. J. Chadi, Phys. Rev. Lett. **82**, 113 (1999).

[12] J. Nissila, K. Saarinen, P. Hautojarvi, A. Suchocki, and J. M. Langer, Phys. Rev. Lett. **82**, 3276 (1999).

[13] A. I. Ritus *et al.* (unpublished).

[14] S. A. Kazanskii, D. S. Rumyantsev, and A. I. Ryskin (unpublished).

[15] S. A. Kazanskii, Pis'ma Zh. Eksp. Teor. Fiz. **38**, 430 (1983) [JETP Lett. **38**, 521 (1983)]; Zh. Eksp. Teor. Fiz. **89**, 1258 (1985) [Sov. Phys. JETP **62**, 727 (1985)]; Pis'ma Zh. Eksp. Teor. Fiz. **41**, 185 (1985) [JETP Lett. **41**, 224 (1985)].

[16] J. P. Laval, A. Abaous, B. Frit, and A. Le Bail, J. Solid State Chem. **85**, 133 (1990).

[17] P. Lagassie, J. Grannee, and J.-M. Ress, Rev. Chim. Miner. **34**, 328 (1987).

[18] S. P. Ivanov, I. I. Buchinskaya, and P. P. Fedorov, Inorg. Mater. (Transl. of Neorg. Mater.) **36**, 484 (2000).

[19] The weakly reducing atmosphere at the crystal growth is stipulated by graphite crucibles, in which the growth takes place.

[20] Au contacts from Schottky barriers on the $CdF_2$ surface [R. Mach and E. U. Messerschmidt, Phys. Status Solidi A **42**, L187 (1977); J. Garbarczyk, B. Krukowska-Fulde, T. Langer, and J. M. Langer, J. Phys. D: Appl. Phys. **11**, L17 (1978)]; the same is true for Ag.

[21] A. Hippel, *Dielectrics and Waves* (Willey, NY, 1954).

[22] I. Kunze and W. Ulrici, Phys. Status Solidi B **55**, 567 (1973).

[23] U. Piekara, J. M. Langer, and U. Krukowska-Fulde, Solid State Commun. **23**, 583 (1977).

[24] Therefore overstated values of binding energy of the shallow centers, $E_{sh}$ of 0.151 eV (Ref. 22) and 0.140 eV (Ref. 23) were found in these studies.

[25] C. H. Champness, Proc. Phys. Soc. London, Sect. B **69**, 1335 (1958).

[26] F. Moser, D. Matz, and S. Lyu, Phys. Rev. **182**, 808 (1969).

[27] J. M. Langer, T. Langer, G. L. Pearson, B. Krukowska-Fulde, and U. Piekara, Phys. Status Solidi B **66**, 537 (1974).

[28] K. G. Lynn (private communication).

[29] Mobility of electrons in $CdF_2$ weakly depends on $T$ in the range $130\ \mathrm{K} \leqslant T \leqslant 230\ \mathrm{K}$ [R. P. Khosla and D. Matz, Solid State Commun. **6**, 859 (1968)] therefore, one may suppose that in this range the $G_1(T)$ dependence is practically determined by the $n(T)$ dependence.

[30] I. Kunze and P. Muller, Phys. Status Solidi A **13**, 197 (1972).